IET Microwaves, Antennas & Propagation

Research Article

IET Journals
The Institution of Engineering and Technology

Gain-enhanced EH_1-mode microstrip leaky-wave antenna with periodical loading of shorting pins

ISSN 1751-8725
Received on 1st June 2017
Revised 15th September 2017
Accepted on 19th October 2017
E-First on 3rd January 2018
doi: 10.1049/iet-map.2017.0459
www.ietdl.org

Danpeng Xie[1] ✉, Lei Zhu[1], Xiao Zhang[1], Neng-Wu Liu[1]

[1]Department of Electrical and Computer Engineering, Faculty of Science and Technology, University of Macau, Macau, People's Republic of China

✉ *E-mail: yb57471@umac.mo*

Abstract: A gain-enhanced EH_1-mode microstrip leaky-wave antenna (MLWA) with periodical loading of shorting pins to improve the radiation gain is proposed. Owing to the equivalent shunt inductive effect of the periodically installed shorting pins, the cut-off frequency of the proposed pin-loaded EH_1-mode microstrip line (MSL) is effectively tuned up; in other words, the lateral electric dimension of the proposed MLWA is effectively enlarged. Therefore, the distance of a pair of in-phase equivalent magnetic-current line sources in two sides of the MSL is widened, resulting to increase the radiation gain of the proposed MLWA. For the sake of theoretical explanation, an analytical model is built up for analysis. Then, numerical investigation is executed to reveal the effect of pins position on the tuning ratio of both the EH_1-mode cut-off frequencies and strip widths. After extensive analysis, a pin-loaded EH_1-mode MLWA under width tuning ratio of 1.78 and periodicity of 10.0 mm is designed, fabricated, and tested. Simulated and measured results both demonstrate that the radiation gain could be successfully raised up from 10.1 dBi (conventional EH_1-mode MLWA) to 13.1 dBi (the proposed pin-loaded one) at the same operating frequency of 4.0 GHz.

1 Introduction

Microstrip leaky-wave antennas (MLWAs) have been widely developed since the first MLWA prototype was demonstrated by Menzel [1]. It exhibits a frequency-dependent steerable beam scanning under the first higher-order EH_1 mode of a microstrip line (MSL). Afterwards, a large number of researchers have been attracted to study and explore these MLWAs [2–10] for a variety of applications in Doppler radar, target tracking, cruise control, and collision avoidance system etc., due to their attractive features, inclusive of planar configuration, easy integration with other integrated circuits, and frequency-dependent beam-scanning ability.

Among their numerous characteristics, the radiation pattern is crucially important and it usually needs to be appropriately reshaped under some prescribed specifications. For example, a broad-beam pattern is realised by either tapering the complex propagation constants along a straight LW structure, or bending a leaky-line at the expense of its directivity [11, 12]. Oppositely, optimum focusing pattern is implemented with the tapering technology, as demonstrated in a width-tapered EH_1-mode MSL [13]. Besides, more diverse radiation patterns are achieved by pattern synthesis technology such as fast Fourier transform [17], transmission line model [19], generalised array factor approach [20], and other analytical approaches [15, 18]. As a result, desired radiation nulls are deliberately produced at certain directions by both properly tapering the illumination [14] and manipulating the effective radiation sections [18]. Moreover, unwanted high sidelobe levels are enormously suppressed by synthesising the illumination distributions [15, 19]. Special distributions such as Taylor or Cosine distribution are demonstrated to be capable to generate a high directivity with extremely low sidelobe levels [16, 20].

Although the above works have achieved their intended targets, these studies mainly focus on characterisation of their radiation patterns in the longitudinal plane through the complex propagation constants. Until now, very few works have been reportedly conducted to characterise their radiation pattern in the transverse plane for effective adjustment of their transverse beamwidth. As it comes to an LWA array with the requirement to improve its directivity for high-gain beam scanning as studied in [21, 22], it is highly demanded to explore the radiation pattern or directivity in the transverse plane of these MLWAs. For this purpose, our work herein will be primarily concentrated on the radiation pattern in the transverse plane, aiming to realise the gain enhancement of the EH_1-mode MLWA.

To do it, the pin-loaded technology is utilised here in the design of a gain-enhanced EH_1-mode MLWA. As reported in [23, 24], shunt inductive effect of shorting pins perturbing the field distribution beneath the patch has successfully enlarged the radiation area at resonance, resulting to improve the directivity of a single patch antenna. From this perspective, the periodical loading of shorting pins [9] could be similarly implemented in an EH_1-mode MLWA to widen its electrical strip width under its transverse resonance. As such, the enlarged distance between two in-phase parallel magnetic-current line sources under the EH_1-mode operation with widened strip width could facilitate us to effectively narrow the radiation beamwidth in the transverse plane for enhancement of radiation gain.

Despite that several works have already presented the pin-loaded MLWAs [25–28], our proposed EH_1-mode MLWA is different from them in the aspects of working principle and operation mode. As claimed in [25], the periodic conducting posts actually act as a partially reflective surface, and the distance between two adjacent side edges in the microstrip section has to be less than quarter wavelength in order to avoid the appearance of other unwanted LW modes. In our design, two columns of periodical shorting pins are installed on the conventional EH_1-mode MSL to merely implement shunt inductive effect to widen its lateral strip width without altering the EH_1-mode operation. In parallel, the shorting pins could be freely located in the transverse position of the MSL with no limitation in strip width as concerned in [25–28]. In the following, our work will be focused on description of our proposed technique in gain enhancement of the proposed pin-loaded MLWA, and implementation of a prototype MLWA for experimental demonstration.

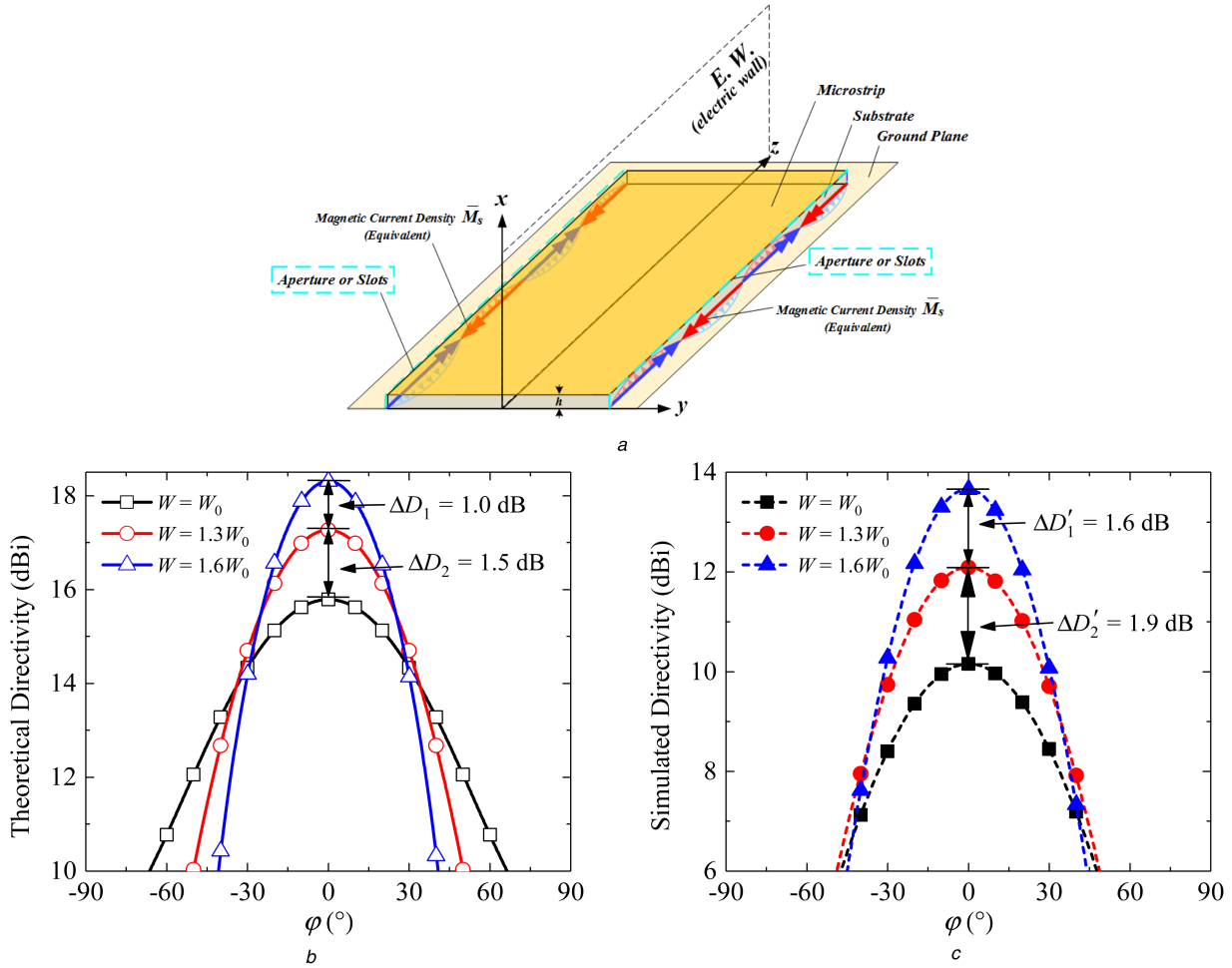

Fig. 1 *Demonstration of the proposed gain-enhanced EH_1-mode MLWA with periodical loading of shorting pins*

(a) Equivalent model with a pair of magnetic-current line sources in two lateral sides of strip conductor, ***(b)*** Theoretical directivity, ***(c)*** Simulated directivity

2 Working principle of gain-enhanced MLWA

According to the Huygens' principle, the radiation pattern of an EH_1-mode MLWA can be equivalently modelled as a two-line array of radiated apertures or slots, as shown in Fig. 1*a*. Considering the longitudinal variation, each magnetic-current line source M_s can be obtained according to their guided-wave phase constant, which is expressed as

$$\bar{M}_s = \hat{z} M_0 \mathrm{e}^{-\mathrm{j}\beta z} = \hat{z}\frac{U_0}{h}\mathrm{e}^{-\mathrm{j}\beta z}, \quad z \in \left[-\frac{L}{2}, \frac{L}{2}\right] \tag{1}$$

where β indicates the phase constant along the MLWA, and it mainly determines the main beam direction.

Therefore, the vector potential F generated by each M_s could be derived as

$$\begin{aligned}\bar{F} &= \frac{1}{4\pi}\int\int_S \frac{\bar{M}_s}{R}\mathrm{e}^{-\mathrm{j}kR}\mathrm{d}S \\ &= \hat{a}_z\frac{\mathrm{e}^{-\mathrm{j}kr}U_0 L}{2\pi r}\mathrm{sinc}(kh\sin\theta\cos\varphi)\mathrm{sinc}\left[\frac{\pi L}{\lambda}\left(\frac{\beta}{k}-\cos\theta\right)\right]\end{aligned} \tag{2}$$

Since the substrate is electrically thin with kh=1, the vector potential F could be simplified as

$$\bar{F} = \hat{a}_z\frac{U_0 L}{2\pi r}\mathrm{e}^{-\mathrm{j}kr}\,\mathrm{sinc}\left[\frac{\pi L}{\lambda}\left(\frac{\beta}{k}-\cos\theta\right)\right] \tag{3}$$

Then, the radiation field excited by the vector potential F is obtained as

$$\begin{aligned}\bar{E} &= -\nabla\times\bar{F} \\ &= -\hat{a}_\varphi \mathrm{j}\frac{U_0 L}{\lambda r}\mathrm{e}^{-\mathrm{j}kr}\,\mathrm{sinc}\left[\frac{\pi L}{\lambda}\left(\frac{\beta}{k}-\cos\theta\right)\right]\sin\theta\end{aligned} \tag{4}$$

Thereby, the total far field generated by these two magnetic-current line sources is derived as

$$\bar{E}_{\mathrm{total}} = 2\bar{E}\mathrm{e}^{\mathrm{j}(1/2)\mathrm{kW}\sin\theta\cos\varphi}\cos\left(\frac{1}{2}\mathrm{kW}\sin\theta\sin\varphi\right) \tag{5}$$

Finally, the normalised radiation pattern $F(\theta, \varphi)$ is expressed as

$$F(\theta,\varphi) = \mathrm{sinc}\left[\frac{\pi L}{\lambda}\left(\frac{\beta}{k}-\cos\theta\right)\right]\cos\left(\frac{\pi W}{\lambda}\sin\theta\sin\varphi\right)\sin\theta \tag{6}$$

Then the total directivity D_t of the two long slots is given by

$$D_t = \frac{U_{\mathrm{Max}}}{U_0} = \frac{4\pi U_{\mathrm{Max}}}{P_{\mathrm{Rad}}} = \frac{\pi(kL)^2}{\int_0^\pi\int_0^\pi [F(\theta,\varphi)]^2\sin\theta\,\mathrm{d}\theta\,\mathrm{d}\varphi} \tag{7}$$

To further describe the width-widening process and illustrate the nature of antenna gain enhancement, the two distinct strip widths before and after loading the shorting pins are denoted as W_0 and W_r in this paper, respectively. Here, the initial value of strip width without shorting pins is set as W_0, which is employed for comparison with the enlarged value of the widened strip width W_r. Meanwhile, the operating frequency of the proposed EH_1-mode MLWA is shifted up from f_0 to f_r, and the effective wavelength varies from λ_0 to λ_r. Under this circumstance, the radiation directivity D_t is basically dependent on all these involved parameters, i.e. f_r/f_0, W_r/W_0, L/λ_0, h/λ_0, and ε_r, such that

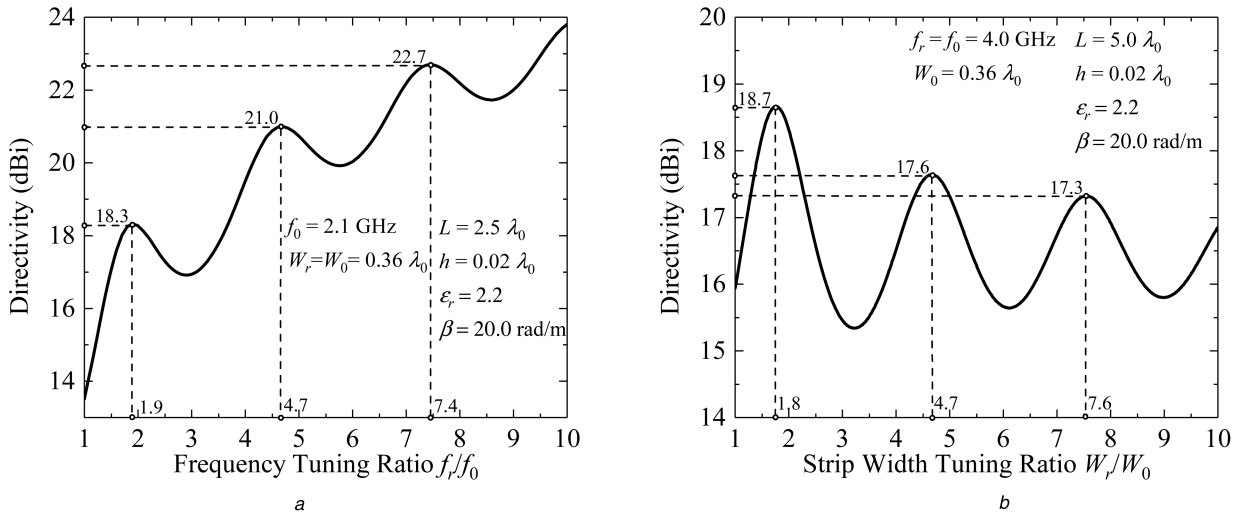

Fig. 2 *Variation in radiation directivity of the EH_1-mode MLWA*

(a) Directivity variation as a function of tuning ratio of operation frequencies f_r/f_0 under the same strip width, ***(b)*** Directivity variation as a function of tuning ratio of strip widths W_r/W_0 at the same operating frequency

$$F(\theta, \varphi) = \operatorname{sinc}\left[\pi \frac{L}{\lambda_0}\frac{f_r}{f_0}\left(\frac{\beta}{k} - \cos\theta\right)\right] \cdot \cos\left(\pi \frac{W_r}{W_0}\frac{f_r}{f_0}\frac{1}{2\sqrt{\varepsilon_e}} \sin\theta \sin\varphi\right) \sin\theta \tag{8}$$

$$\varepsilon_e = \frac{\varepsilon_r + 1}{2} + \frac{\varepsilon_r - 1}{2}\left[1 + 12\frac{h}{\lambda_0}\frac{\lambda_0}{L}\right]^{-1/2} \tag{9}$$

In design, the relative permittivity ε_r and substrate height h/λ_0 of a dielectric substrate are readily settled when a substrate is selected. Meanwhile, the longitudinal length of an LWA L/λ_0 is always selected long enough for better efficient radiation. Thereafter, the radiation directivity D_t is primarily decided by two key parameters f_r/f_0, W_r/W_0.

Regardless that these two parameters give their distinctive effects on the directivity variation, it is the lateral electrical strip width of this EH_1-mode MLWA to determine its radiation directivity. For an intuitive illustration, the transverse radiation patterns under varied strip widths are graphically provided for comparative demonstration of this gain-enhanced property. As shown in Fig. 1*b*, the theoretical directivity is increased from 15.8, 17.3 to 18.3 dBi with the increments of $\Delta D_2 = 1.5$ dB and $\Delta D_1 = 1.0$ dB, respectively, as the strip width extends from W_0, 1.3, W_0 to 1.6 W_0 under the same operating frequency of 4.0 GHz. The pin-loaded microstrip structure under the selection of $N = 36$, $T = 10.0$ mm is then simulated, as shown in Fig. 1*c*. In this case, the according directivity enhancement is obtained as $\Delta D'_2 = 1.9$ dB and $\Delta D'_1 = 1.6$ dB. From both calculated and simulated results, it can be seen that the strip width enlargement of MSL plays an important role in directivity increment.

To clearly demonstrate the directivity variation, the theoretical directivities as a function of f_r/f_0 and W_r/W_0 are separately exhibited. Thus, the maximum directivity increment can be acquired for design of the proposed gain-enhanced EH_1-mode MLWA as will be detailed in Sections 3 and 4.

2.1 Varied operation frequencies

Under varied operation frequencies with the fixed electrical strip width, the radiation directivity as a function of the tuning ratio of frequencies f_r/f_0 could be analysed and characterised, where $f_r > f_0$. As can be seen from Fig. 2*a*, the directivity increases in an oscillating way with the first three peaks of 18.3 dBi at $f_r/f_0 = 1.9$, 21.0 dBi at $f_r/f_0 = 4.7$, and 22.7 dBi at $f_r/f_0 = 7.4$, under the condition of $f_0 = 2.1$ GHz, $W_r = W_0 = 0.36\lambda_0$, $L = 2.5\ \lambda_0$, $h = 0.02\lambda_0$, $\varepsilon_r = 2.2$, and $\beta = 20.0$ rad/m.

2.2 Varied strip widths

Under the same operating frequency, the increment of directivity is mainly decided by the tuning ratio of strip widths W_r/W_0, where $W_r > W_0$. As depicted in Fig. 2*b*, the directivity increases in a similar but different oscillating manner under the condition of $f_r = f_0 = 4.0$ GHz, $W_0 = 0.36\lambda_0$, $L = 5.0\lambda_0$, $h = 0.02\lambda_0$, $\varepsilon_r = 2.2$, and $\beta = 20$ rad/m. Its maximum directivity of 18.7 dBi shows up at the first peak with $W_r/W_0 = 1.8$, and the following peaks gradually decrease with their directivities of 17.6 and 17.3 dBi when $W_r/W_0 = 4.7$ and 7.6, respectively. Therefore, Fig. 2*b* reveals that the maximum directivity could be ultimately attained as W_0 is aggrandised to 1.8 W_0.

3 Gain-enhanced pin-loaded EH_1-mode MLWA

With the above-described analysis, the working principle of our proposed gain-enhanced MLWA can be clearly explicated. To realise the maximum directivity enhancement as desired, it is essential to acquire the widened strip width with tuning ratio of strip widths $W_r/W_0 = 1.8$ under the operating frequency of 4.0 GHz. To do it, our developed pin-loaded technique [23, 24] is implemented to widen the strip width toward design of the width-widened EH_1-mode MLWA.

The proposed EH_1-mode MLWA is comprised up by symmetrically installing two columns of shorting pins at two sides of its central plane as shown in Fig. 3*b*. As compared with the conventional MLWA in Fig. 3*a*, the proposed one is maintained to operate under the EH_1-mode propagation. Their symmetrical planes, as marked in dash lines, function as the electric wall (EW), where the electric fields reverse their phases once. As the two key parameters, the proposed pin-loaded EH_1-mode MLWA structure has the longitudinal periodicity T and lateral distance P between the two columns of shorting pins. They work together to determine the cut-off frequency and the widened strip width of the EH_1-mode MLWA. In the following, the effect of the pins position P/W_r under varied periodicities T on the tuning ratio of frequencies f_r/f_0 and strip widths W_r/W_0 will be explicitly investigated, aiming to thoroughly reveal the gain-enhanced property of the proposed pin-loaded EH_1-mode MLWA.

3.1 Pins position P/W_r effect on f_r/f_0

To acquire the tuning ratio of frequencies f_r/f_0 under varied pins positions P/W_r and periodicities T, the so-called high frequency structure simulator (HFSS)-short-open-load (SOL) numerical method [29] is applied to extract the operating frequency. This

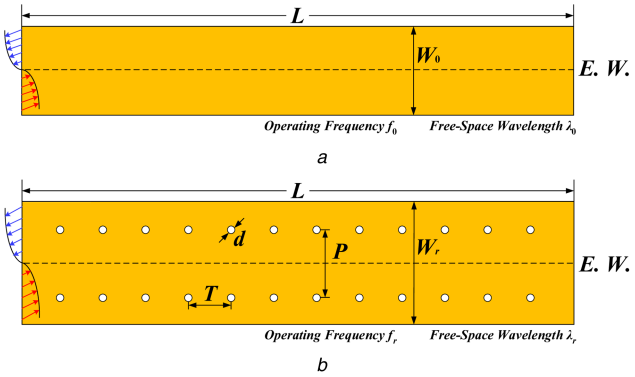

Fig. 3 *Top view of the EH$_1$-mode MLWAs with and without two columns of periodic shorting pins*
(a) Conventional EH$_1$-mode MLWA, ***(b)*** Proposed EH$_1$-mode MLWA with periodical loading of shorting pins

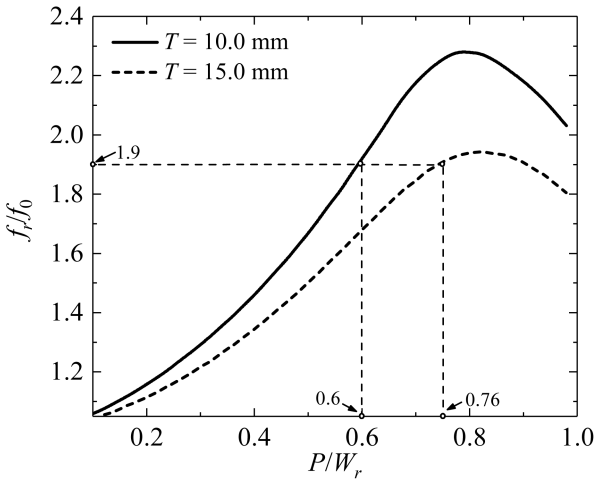

Fig. 4 *Tuning ratio of operation frequencies f_r/f_0 as a function of pins position P/W_r under the same strip width of $W_r = W_0 = 45.0$ mm*

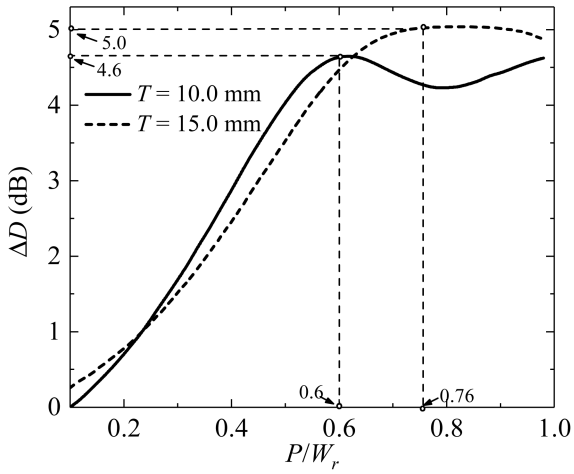

Fig. 5 *Directivity increment ΔD as a function of pins position P/W_r under the same strip width of $W_r = W_0 = 45.0$ mm*

method is stemmed from the SOC calibration method [30]. It needs to be mentioned herein that the cut-off frequency is selected as the operating frequency for the purpose of large leakage constant or high radiation efficiency. Under the same condition in Fig. 2*a* with $f_0 = 2.1$ GHz, the numerically extracted strip width here is unchanged as $W_r = W_0 = 45.0$ mm. In this way, f_r/f_0 corresponding to varied P/W_r is obtained as depicted in Fig. 4. It can be clearly seen herein that f_r/f_0 reaches to the value of 1.9 as P/W_r approaches to 0.6 for $T = 10.0$ mm and 0.76 for $T = 15.0$ mm, and it is the first peak in directivity as predicted in Fig. 2*a*. With reference to the

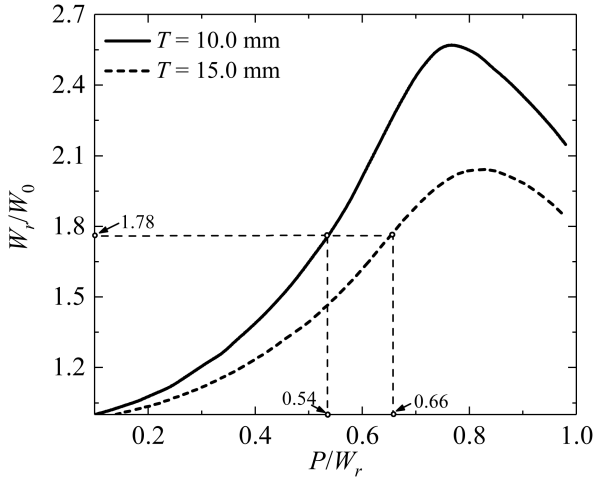

Fig. 6 *Tuning ratio of strip widths W_r/W_0 as a function of pins position P/W_r under the same operating frequency of $f_r = f_0 = 4.0$ GHz*

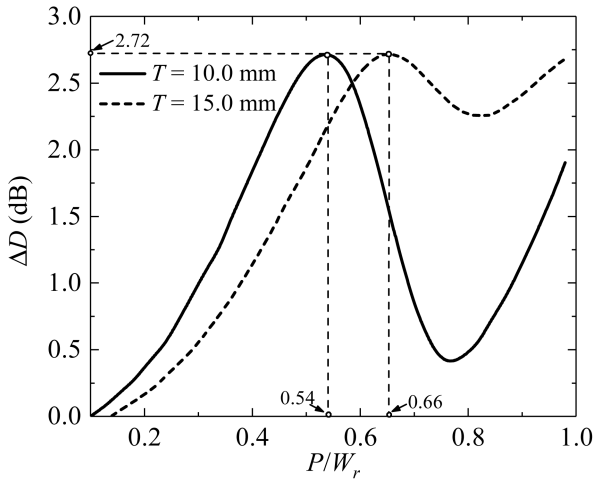

Fig. 7 *Directivity increment ΔD as a function of pins position P/W_r under the same operating frequency of $f_r = f_0 = 4.0$ GHz*

calculated value of directivity in Fig. 2*a*, the directivity increment ΔD as a function of P/W_r could be realised, as shown in Fig. 5.

3.2 Pins position P/W_r effect on W_r/W_0

Similarly, the tuning ratio of strip widths W_r/W_0 under varied pins positions P/W_r and periodicities T could be explored for the same purpose. Herein, the same condition as indicated in Fig. 2*b* with the unchanged operating frequency of $f_r = f_0 = 4.0$ GHz is implemented. Consequently, the numerically extracted strip width is gradually enlarged from the initial value of $W_0 = 22.5$ mm to W_r. As shown in Fig. 6, W_r/W_0 reaches to 1.78 when P/W_r approaches to 0.54 for $T = 10.0$ mm and 0.66 for $T = 15.0$ mm, and it is approximately equal to the calculated value of 1.8 at the position of peak directivity as predicted in Fig. 2*b*. With reference to the calculated value of directivity in Fig. 2*b*, the directivity increment ΔD as a function of P/W_r could be achieved, as shown in Fig. 7.

On the basis of the results provided above, one can figure out that under the same operating frequency of 4.0 GHz, the strip width W_r of the proposed EH$_1$-mode MLWA can be enlarged to 1.78 times wider than the conventional counterpart W_0, i.e. $W_r/W_0 = 1.78$, when P/W_r equals to 0.54 for $T = 10.0$ mm or 0.66 for $T = 15.0$ mm. As a consequence, the maximum directivity increment of 2.7 dB could be finally actualised in theoretical calculation.

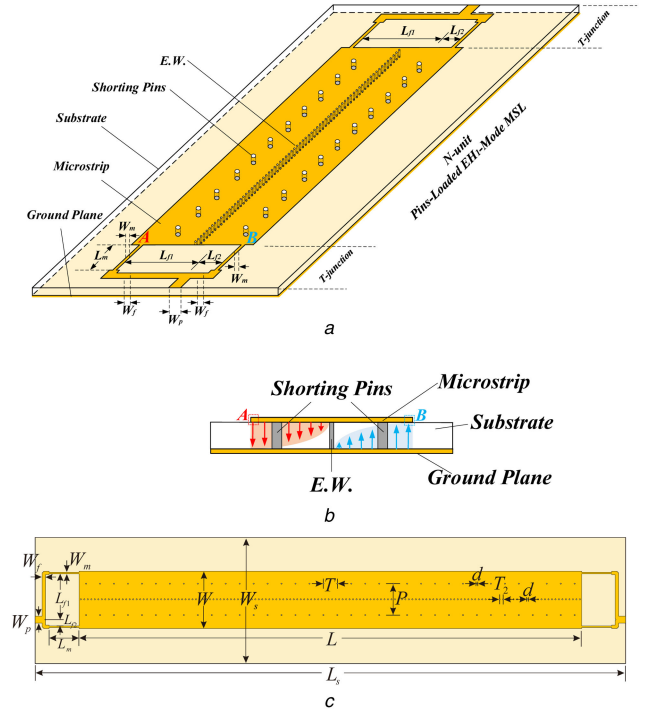

Fig. 8 *Configuration of the proposed gain-enhanced EH1-mode MLWA with periodically loading of shorting pins*
(a) 3D geometry, ***(b)*** Side view, ***(c)*** Top view

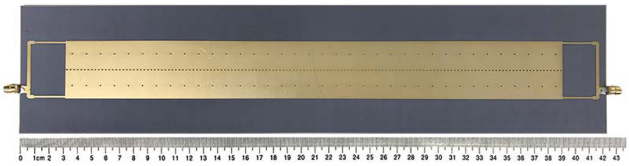

Fig. 9 *Photograph of the fabricated MLWA prototype*

4 Design, implementation, and measurement

Following the above discussion, an antenna prototype with $P/W_r = 0.54$, $T = 10.0$ mm, and $W_r/W_0 = 1.78$, is subsequently designed. The three-dimensional (3D) configuration of the proposed pin-loaded EH1-mode MLWA is depicted in Fig. 8*a*. It is comprised of a section with N-unit pin-loaded EH_1-mode microstrip structure in the middle and two T-junction sections at two terminals. The whole antenna is designed on poly tetra fluoroethylene plus woven glass (F4B), substrate with relative permittivity of 2.2, dielectric loss tangent of 0.001, and thickness of 1.6 mm. The N-unit MSL structure is periodically loaded with $2 \times N$ shorting pins with periodicity of T and lateral distance of P, and it is terminated at its two ends with the standard quarter-wavelength MSL impedance transformers with length L_m and strip width W_m. For satisfactory mode matching and good excitation of EH_1-mode, the points A and B at the edges of the MSL are connected by the two branch lines with differential feeding. Consequently, the length of the two branch lines has to satisfy the phase condition of $L_{f1} - L_{f2} = \pi/\beta_m$, where β_m is the phase constant of EH_0-mode microstrip feeding line. Besides, the centreline of the EH_1-mode MLWA is installed with a column of closely spaced shorting pins with periodicity of T_2 as shown in Fig. 8*c* to function as an EW to ensure the EH1-mode operation.

By using the full-wave electromagnetic simulator HFSS, the proposed antenna prototype is simulated and the optimised dimension parameters in Fig. 8*c* are listed in Table 1. Afterwards, the antenna prototype is fabricated for test, and the photograph of the fabricated antenna is shown in Fig. 9. By using the R&S ZNB-20 Vector Network Analyser, its reflection coefficient is measured as depicted in Fig. 10*a*. The measured results in dash line are found in good accordance with the simulated results, and both

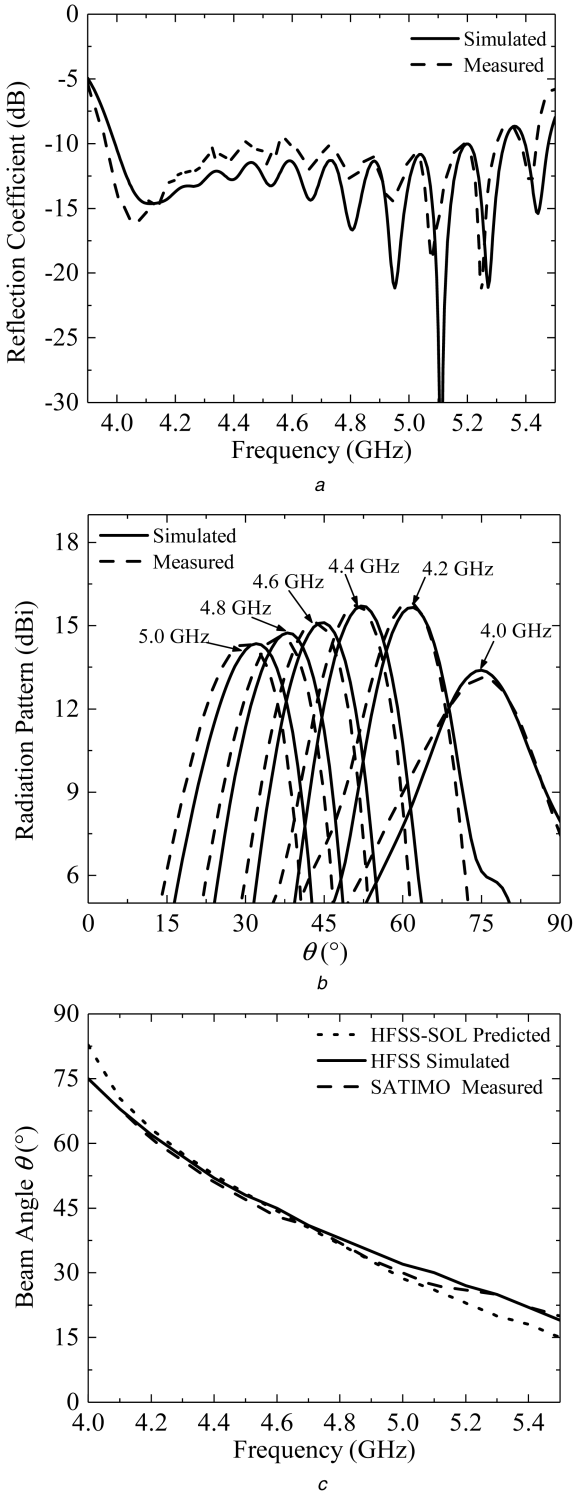

Fig. 10 *Test results of the proposed EH_1-mode MLWAs prototypes*
(a) Simulated and measured reflection coefficients, ***(b)*** Simulated and measured longitudinal radiation patterns, ***(c)*** Simulated and measured beam angle θ

of them are maintained lower than −10 dB in the LW region from 4.0 to 5.15 GHz. By using the StarLab Société d'Applications Technologiques de l'Imagerie Micro-Onde (SATIMO) measurement system, its radiation performance is then measured. Fig. 10*b* shows the simulated and measured longitudinal radiation patterns from 4.0 to 5.0 GHz. Fig. 10*c* summarises the beam-scanning angles θ. It can be seen herein that the proposed antenna could achieve a wide beam-scanning scale from $\theta = 75°$ at 4.0 GHz to $\theta = 20°$ at 5.5 GHz. Again, the measured results are found in good agreement with the predicted results from the SOL-HFSS extraction approach.

Table 1 Final parameters of the designed gain-enhanced EH1-mode MLWA

Parameter, mm	Value	Parameter, mm	Value	Parameter, mm	Value
W_m	1.25	W_s	90.0	T	10.0
L_m	21.5	L_s	423.0	T_2	2.5
W_p	5.0	W_r	40.9	P	21.6
L_{f1}	32.7	L	360.0	d	0.8
L_{f2}	4.5	W_f	2.5	N	36

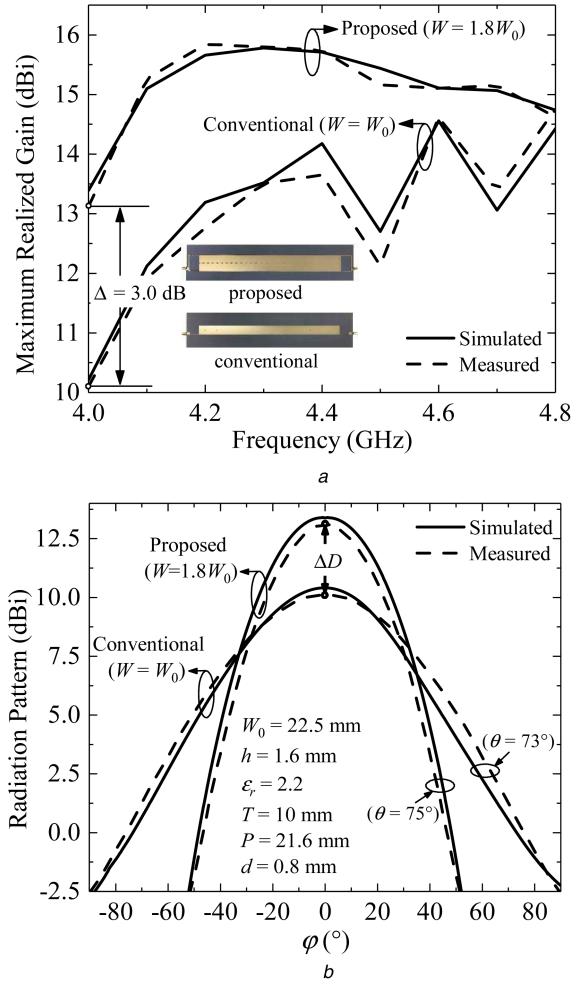

Fig. 11 *Maximum realised gains and transverse radiation patterns of the proposed width-widened antenna with $W = 1.8W_0$, in comparison with the conventional one with $W = W_0$*

(a) Simulated and measured maximum realised gains, ***(b)*** Simulated and measured transverse radiation patterns at 4.0 GHz

For better illustration of the gain-enhanced property of the proposed antenna, a conventional EH_1-mode MLWA with no pin-loaded technique is implemented as well for comparative study. It can be observed from Fig. 11*a* that a 3.0 dB increment in the maximum realised gain at 4.0 GHz is realised, which evidently proves the validation of the theoretical analysis. However, as the frequency increases, the increment is gradually reduced. This phenomenon could be intuitively explained by the theoretical results in Fig. 2*b*. For the conventional antenna, the enlarged electrical dimension ($W_0 < W_r < 1.8\ W_0$) in the higher frequency can gradually increase the directivity than the conventional one with the strip width W_0. For the proposed antenna, the over-enlarged electrical dimension will hardly further enhance the directivity as $W_r > 1.8\ W_0$ is selected. Nevertheless, the proposed pin-loaded technique applied in EH_1-mode MLWAs could effectively widen the strip width in a flexible scale, thus to enhance the directivity to a desired extent. Finally, the simulated and measured transverse radiation patterns at 4.0 GHz are displayed in Fig. 11*b*. It clearly exhibits that the transverse beamwidth of the proposed antenna is tremendously narrowed as compared with its conventional counterpart, thereby exposing the innate reason of the directivity enhancement.

5 Conclusion

In this paper, a class of gain-enhanced EH_1-mode MLWAs with periodical loading of shorting pins is proposed, designed, and implemented. After installing the two columns of periodic shorting pins, its strip width can be properly widened under the EH_1-mode operation to enlarge the distance between two in-phase parallel magnetic-current line sources at its two lateral sides, resulting to enhance its radiation directivity. After its working principle is described, numerical extraction on its LW parameters is executed to reveal the pins effect on the tuning ratios of cut-off frequencies and strip widths. According to the derived results, a set of key parameters with maximum theoretical directivity increment is applied for design and implementation of the proposed EH_1-mode MLWA fed by MSLs at its two terminals. Simulated and measured results both verify the proposed design concept and predicted directivity increment.

6 Acknowledgments

This work was supported in part by the National Natural Science Foundation of China through the General Program under grant no. 61571468, in part by the Macao Science and Technology Development Fund through the FDCT Research Grant under grant no. 091/2016/A2, in part by the University of Macau through the CPG Research Grant under grant no. CPG2017-00028-FST, and the Multi-Year Research Grant under grant no. MYRG2017-00007-FST.

7 References

[1] Menzel, W.: 'A new traveling-wave antenna in microstrip', *Arch. Elektr. Übertrag. Tech.*, 1979, **33**, pp. 137–140

[2] Oliner, A.A.: 'Leakage from higher modes on microstrip line with application to antenna', *Radio Sci.*, 1987, **22**, (6), pp. 907–912

[3] Oliner, A.A.: 'Scannable millimeter wave arrays, volume II'. Final Technical Report, Polytechnic University, Farmingdale, NY, April 1989, pp. 304–315

[4] Bhattacharyya, A.K.: 'Long rectangular patch antenna with a single feed', *IEEE Trans. Antennas Propag.*, 1990, **38**, (7), pp. 987–993

[5] Lin, Y.-D., Sheen, J.-W., Tzuang, C.-K.C.: 'Analysis and design of feeding structures for microstrip leaky-wave antenna', *IEEE Trans. Antennas Propag.*, 1996, **44**, (9), pp. 1540–1547

[6] Qian, Y., Chang, B., Itoh, T., *et al.*: 'High efficiency and broadband excitation of leaky mode in microstrip structures'. Proc. IEEE Microwave Theory and Techniques Digest, Anaheim, CA, June 1999, pp. 1419–1422

[7] Hong, W., Chen, T., Chang, C., *et al.*: 'Broadband tapered microstrip leaky-wave antenna', *IEEE Trans. Antennas Propag.*, **51**, (8), pp. 1922–1928

[8] Zelinski, G.M., Thiele, G.A., Hastriter, M.L., *et al.*: 'Half width leaky-wave antennas', *IET Microw. Antennas Propag.*, 2007, **1**, (2), pp. 341–348

[9] Xie, D., Zhu, L., Zhang, X.: 'An EH_0-mode microstrip leaky-wave antenna with periodical loading of shorting pins', *IEEE Trans. Antennas Propag.*, **65**, (7), pp. 3419–3426

[10] Liu, J., Li, Y., Long, Y.: 'Design of periodic shorting-vias for suppressing the fundamental mode in microstrip leaky-wave antennas', *IEEE Trans. Antennas Propag.*, 2015, **63**, (10), pp. 4297–4304

[11] Burghignoli, P., Frezza, F., Galli, A., *et al.*: 'Synthesis of broadbeam patterns through leaky-wave antennas with rectilinear geometry', *IEEE Antennas Wirel. Propag. Lett.*, **2**, pp. 136–139

[12] Ohtera, I.: 'Diverging/focusing of electromagnetic waves by utilizing the curved leakywave structure: application to broad-beam antenna for radiating within specified wide-angle', *IEEE Trans. Antennas Propag.*, **47**, (9), pp. 1470–1475

[13] Gómez-Tornero, J.L.: 'Analysis and design of conformal tapered leakywave antennas', *IEEE Antennas Wirel. Propag. Lett.*, **10**, pp. 1068–1071

[14] Martinez-Ros, A.J., Gómez-Tornero, J.L., Clemente-Fernández, F.J., *et al.*: 'Microwave near-field focusing properties of width-tapered microstrip leaky-wave antenna', *IEEE Trans. Antennas Propag.*, **61**, (6), pp. 2981–2990
[15] Li, Z., Wang, J.H., Zhang, Z., *et al.*: 'Far field computation of the traveling wave structures and a new approach for suppressing the sidelobe levels', *IEEE Trans. Antennas Propag.*, **61**, (4), pp. 2308–2312
[16] Liu, J., Jackson, D., Li, Y., *et al.*: 'Investigations of SIW leaky-wave antenna for endfire radiation with narrow beam and sidelobe suppression', *IEEE Trans. Antennas Propag.*, **62**, (9), pp. 4489–4497
[17] Gómez-Tornero, J.L., Martinez-Ros, A.J., Verdú-Monedero, R.: 'FFT synthesis of radiation patterns with wide nulls using tapered leaky-wave antennas', *IEEE Antennas Wirel. Propag. Lett.*, **9**, pp. 518–521
[18] Li, Z., Wang, J.H., Chen, M., *et al.*: 'New approach of radiation pattern control for leaky-wave antennas based on the effective radiation sections', *IEEE Trans. Antennas Propag.*, **63**, (7), pp. 2867–2878
[19] Nguyen-Trong, N., Hall, L., Fumeaux, C.: 'Transmission-line model of nonuniform leaky-wave antennas', *IEEE Trans. Antennas Propag.*, **64**, (3), pp. 883–893
[20] Rance, O., Lemaître-Auger, P., Siragusa, R., *et al.*: 'Generalized array factor approach to the assessment of discrete tapered nonuniform leaky-wave antenna', *IEEE Trans. Antennas Propag.*, **63**, (9), pp. 3868–3877
[21] Hu, C., Tzuang, C.: 'Microstrip leaky-mode antenna array', *IEEE Trans. Antennas Propag.*, **45**, (11), pp. 1698–1699
[22] Hu, C., Tzuang, C.: 'Analysis and design of large leaky-mode array employing the coupled-mode approach', *IEEE Trans. Microw. Theory Tech.*, **49**, (4), pp. 629–636
[23] Zhang, X., Zhu, L.: 'Gain-enhanced patch antennas with loading of shorting pins', *IEEE Trans. Antennas Propag.*, **64**, (8), pp. 3310–3318
[24] Zhang, X., Zhu, L.: 'High-gain circularly polarized microstrip patch antenna with loading of shorting pins', *IEEE Trans. Antennas Propag.*, **64**, (6), pp. 2172–2178
[25] Martinez-Ros, A.J., Gómez-Tornero, J.L., Goussetis, G.: 'Planar leaky-wave antenna with flexible control of the complex propagation constant', *IEEE Trans. Antennas Propag.*, **60**, (3), pp. 1625–1630
[26] Martinez-Ros, A.J., Gómez-Tornero, J.L., Quesada-Pereira, F.: 'Efficient analysis and design of novel SIW leaky-wave antenna', *IEEE Antennas Wirel. Propag. Lett.*, **12**, pp. 496–499
[27] Martinez-Ros, A.J.: 'Holographic pattern synthesis with modulated SIW line-source leaky-wave antennas', *IEEE Trans. Antennas Propag.*, **61**, (7), pp. 3466–3474
[28] Martinez-Ros, A.J., Gómez-Tornero, J.L., Goussetis, G.: 'Conformal tapered substrate integrated waveguide leaky-wave antenna', *IEEE Trans. Antennas Propag.*, **62**, (12), pp. 5983–5991
[29] Wu, Q., Zhu, L.: 'Numerical de-embedding of effective wave impedances of substrate integrated waveguide with varied via-to-via spacings', *IEEE Microw. Wirel. Compon. Lett.*, **26**, (1), pp. 1–3
[30] Zhu, L., Wu, K.: 'Unified equivalent-circuit model of planar discontinuities suitable for field theory based CAD and optimization of M(H)MIC's', *IEEE Trans. Microw. Theory Tech.*, **47**, (9), pp. 1589–1602